

Available online at [www.sciencedirect.com](http://www.sciencedirect.com)

ScienceDirect

Journal homepage: [www.elsevier.com/locate/cortex](http://www.elsevier.com/locate/cortex)

## Research Report

# Distinct sensitivities of the lateral prefrontal cortex and extrastriate body area to contingency between executed and observed actions

Q10

Q9

Akihiro T. Sasaki <sup>a,b,c,d,1</sup>, Yuko Okamoto <sup>e,f,1</sup>, Takanori Kochiyama <sup>e</sup>,  
Ryo Kitada <sup>g,\*</sup> and Norihiro Sadato <sup>a,h,i</sup>

Q1

<sup>a</sup> National Institute for Physiological Sciences, Okazaki, Aichi, Japan

<sup>b</sup> Pathophysiological and Health Science Team, RIKEN Center for Life Science Technologies, Kobe, Hyogo, Japan

<sup>c</sup> Laboratory for Pathophysiological and Health Science, RIKEN Center for Biosystems Dynamics Research, Kobe, Hyogo, Japan

<sup>d</sup> Health Evaluation Team, RIKEN Compass to Healthy Life Research Complex Program, Kobe, Hyogo, Japan

<sup>e</sup> ATR-Promotions, Brain Activity Imaging Center, Kyoto, Japan

<sup>f</sup> Research Center for Child Mental Development, University of Fukui, Yoshida, Fukui, Japan

<sup>g</sup> School of Social Sciences, Nanyang Technological University, Singapore

<sup>h</sup> Division of Physiology, Department of Life Science, The Graduate University of Advanced Study (SOKENDAI), Okazaki, Aichi, Japan

<sup>i</sup> Biomedical Imaging Research Center, University of Fukui, Yoshida, Fukui, Japan

Q2

## ARTICLE INFO

## Article history:

Received 11 January 2018

Reviewed 10 February 2018

Revised 23 April 2018

Accepted 2 August 2018

Action editor Gereon Fink

Published online xxx

## Keywords:

Social contingency

Being imitated

Agency

Body ownership

Action observation network

## ABSTRACT

Detecting relationships between our own actions and the subsequent actions of others is critical for our social behavior. Self-actions differ from those of others in terms of action kinematics, body identity, and feedback timing. Thus, the detection of social contingency between self-actions and those of others requires comparison and integration of these three dimensions. Neuroimaging studies have highlighted the role of the frontotemporal network in action representation, but the role of each node and their relationships are still controversial. Here, we conducted a functional MRI experiment to test the hypothesis that the lateral prefrontal cortex and lateral occipito-temporal cortex are critical for the integration processes for social contingency. Twenty-four adults performed right finger gestures and then observed them as feedback. We manipulated three parameters of visual feedback: action kinematics (same or different gestures), body identity (self or other), and feedback timing (simultaneous or delayed). Three-way interactions of these factors were observed in the left inferior and middle frontal gyrus (IFG/MFG). These areas were active when self-actions were directly fed back in real-time (i.e., the condition causing a sense of

**Abbreviations:** CDM, contingency detection module; EBA, extrastriate body area; SNC, Self/No-Delay/Concordant; ONC, Other/No-Delay/Concordant; SND, Self/No-Delay/Discordant; OND, Other/No-Delay/Discordant; SDC, Self/Delay/Concordant; ODC, Other/Delay/Concordant; SDD, Self/Delay/Discordant; ODD, Other/Delay/Discordant; IFG, inferior frontal gyrus; MFG, middle frontal gyrus; SPL, superior parietal lobule; PreCG, precentral gyrus; ITG, inferior temporal gyrus; MTG, middle temporal gyrus; PostCG, postcentral gyrus; SFG, superior frontal gyrus; IPL, inferior parietal lobule; ASD, autism spectrum disorders.

\* Corresponding author. School of Social Sciences, Nanyang Technological University, 14 Nanyang Avenue, 637332, Singapore.

E-mail address: [ryokitada@ntu.edu.sg](mailto:ryokitada@ntu.edu.sg) (R. Kitada).

<sup>1</sup> These authors contributed equally to the work of this manuscript.

<https://doi.org/10.1016/j.cortex.2018.08.003>

0010-9452/© 2018 The Author(s). Published by Elsevier Ltd. This is an open access article under the CC BY-NC-ND license (<http://creativecommons.org/licenses/by-nc-nd/4.0/>).

Please cite this article in press as: Sasaki, A. T., et al., Distinct sensitivities of the lateral prefrontal cortex and extrastriate body area to contingency between executed and observed actions, *Cortex* (2018), <https://doi.org/10.1016/j.cortex.2018.08.003>

agency), and when participants observed gestures performed by others after a short delay (i.e., the condition causing social contingency). In contrast, the left extrastriate body area (EBA) was sensitive to the concordance of action kinematics regardless of body identity or feedback timing. Body identity  $\times$  feedback timing interactions were observed in regions including the superior parietal lobule (SPL). An effective connectivity analysis supported the model wherein experimental parameters modulated connections from the occipital cortex to the IFG/MFG via the EBA and SPL. These results suggest that both social contingency and the sense of agency are achieved by hierarchical processing that begins with simple concordance coding in the left EBA, leading to the complex coding of social relevance in the left IFG/MFG.

© 2018 The Author(s). Published by Elsevier Ltd. This is an open access article under the CC BY-NC-ND license (<http://creativecommons.org/licenses/by-nc-nd/4.0/>).

## Q3 1. Introduction

Humans can recognize the relationships between self-actions and their consequences during social interactions—a cause-effect representation referred to as social contingency (Gergely, 2001; Nadel, 2002). Social contingency is considered a basic element of the development of social communication skills (Contaldo, Colombi, Narzisi, & Muratori, 2016) and is known to influence the social behavior of adults (Ashton-James, van Baaren, Chartrand, Decety, & Karremans, 2007; van Baaren, Holland, Kawakami, & van Knippenberg, 2004). Although several studies have examined the neural mechanisms underlying social contingency detection in infants (Reid, Striano, & Iacoboni, 2011; Saby, Marshall, & Meltzoff, 2012) and adults (Decety, Chaminade, Grèzes, & Meltzoff, 2002; Guionnet et al., 2012; Kuhn et al., 2010; Okamoto et al., 2014), these mechanisms remain poorly understood. In the present study, we investigated the neural substrates underlying contingency detection between observed and executed actions.

To explain the development of social contingency detection in children, Gergely and Watson (1999) postulated the presence of a “contingency detection module (CDM)”, which functions to establish the primary representation of the bodily self as well as the subsequent orientation toward reactive social objects. This module is innately set to preferentially explore perfect response-contingent stimulation. This perfect contingency includes the relationship between a self-action and its simultaneous visual feedback. Around 3 months of age, the CDM is “switched” toward a preference for less-than-perfectly contingent actions of others, such as the recognition of being imitated (Bahrick & Watson, 1985; Gergely & Watson, 1999). This hypothesis suggests that common mechanisms are involved in perfect and less-than-perfect social contingencies.

Both perfect and less-than-perfect contingencies involve specific relationships between the self-produced and subsequently observed actions of oneself and others. For instance, in perfect contingency, we observe the same action kinematics of our own body at the same timing as the executed action, which leads to the sense of agency. On the other hand, in the case of less-than-perfect contingency (e.g., imitation), we observe another's body movement only after the execution of the self-action, although the action kinematics of the two movements are the same. Thus, contingency detection requires comparison

of executed and observed actions in terms of action kinematics, body identity (self or other), and timing (simultaneous or delayed), as well as the integration of signals reflecting the results of such comparisons. If there is a neural substrate corresponding to the CDM, it should be involved in integrating signals that reflect different aspects of the output/input relationship in both perfect and less-than-perfect contingencies.

Several neuroimaging and electrophysiological studies have aimed to identify the brain networks activated during both action execution and observation (Caspers, Zilles, Laird, & Eickhoff, 2010; Gazzola & Keysers, 2009; Iacoboni & Dapretto, 2006; Molenberghs, Cunnington, & Mattingley, 2012). Previous functional magnetic resonance imaging (fMRI) studies have indicated that the lateral prefrontal cortex (LPFC) and lateral occipito-temporal cortex (LOTc) are involved in the sense of agency (David et al., 2007; Sperduti, Delaveau, Fossati, & Nadel, 2011) and imitation recognition (Decety et al., 2002; Guionnet et al., 2012; Okamoto et al., 2014). The LOTc receives motor input (Astafiev, Stanley, Shulman, & Corbetta, 2004; Orlov, Makin, & Zohary, 2010), while a portion of the extrastriate body area (EBA) within the lateral occipito-temporal cortex is sensitive to imitation (Okamoto et al., 2014) and has been associated with the sense of agency (David et al., 2007). However, the relationships between the LPFC and LOTc are still controversial. It is widely assumed that their relationship is hierarchical, and that the LOTc functions at a relatively lower level (Cattaneo, Sandrini, & Schwarzbach, 2010; Hamilton & Grafton, 2008). On the other hand, more recent neuroimaging studies have shown that the LOTc, rather than frontal regions, is involved in representing actions at the abstract level (Oosterhof, Tipper, & Downing, 2013; Wurm & Lingnau, 2015S), Q4 challenging the conventional view. The relative contributions of these regions to the integration of signals required to detect both perfect and social contingencies remain unknown.

In the present study, we conducted a functional MRI experiment involving healthy adults to determine which brain regions are involved in the integration of signals associated with the relationships between self-produced and subsequently observed actions. The participants performed specific finger movements with the right hand, following which they observed various actions. We manipulated three factors: action kinematics (i.e., categories of finger actions), body identity, and feedback timing. Thus, one of the conditions corresponded to perfect contingency, while another corresponded to less-than-

perfect contingency (i.e., being imitated). To determine which brain regions are involved in the integration of such signals, we examined interactions among the three factors (Calvert, Campbell, & Brammer, 2000; Raij, Uutela, & Hari, 2000; Sumiya, Koike, Okazaki, Kitada, & Sadato, 2017; Takahashi et al., 2015). We hypothesized that interaction effects would be observed in brain regions such as the LPFC and EBA.

## 2. Methods

### 2.1. Participants

Twenty-four healthy volunteers (13 men, mean age:  $24.8 \pm 6.5$  years) participated in the present study. All participants had normal or corrected-to-normal visual acuity, were right handed as determined using the Edinburgh Handedness Inventory (Oldfield, 1971), and were free of neurological or psychiatric illness. The study protocol was approved by the Ethical Committee of the National Institute for Physiological Sciences, Japan. All experiments were conducted in accordance with the Declaration of Helsinki, and all individuals provided written informed consent prior to participation.

### 2.2. Acquisition of imaging data

All functional volumes were acquired using T2\*-weighted gradient-echo echo-planar imaging (EPI) sequences on a 3T MR imager (Allegra, Siemens, Erlangen, Germany). Each volume consisted of 39 3-mm oblique slices covering the entire cerebrum and cerebellum. Axial slices were acquired sequentially in an ascending order. Images were obtained using the following parameters: repetition time (TR) = 2,500 msec; echo time (TE) = 30 msec; flip angle = 80°; field-of-view (FOV) =  $192 \times 192$  mm; pixel dimension =  $3 \times 3$  mm. For each participant, a high-resolution anatomical T1-weighted image was also acquired (voxel dimensions =  $.9 \times .9 \times 1$  mm). Head motion was minimized by placing comfortable but tight-fitting foam padding around each participant's head.

### 2.3. Experimental design

We used a three-factor within-subject factorial design, with two levels in each factor (eight conditions in total). Factors included body identity (Self/Other), feedback timing (Delay/No-delay), and action kinematics (Concordant/Discordant) (Fig. 1a).

The experiment consisted of eight runs. Four runs were used to examine brain activity during the Self conditions (Self runs), while the remaining four were used for the Other conditions (Other runs). Each run contained eight task blocks and nine rest blocks. Task blocks and rest blocks were alternated such that the first rest block was followed by the first task block, while the final task block was followed by the last rest block (Fig. 1c). All task blocks and rest blocks lasted for 20 sec except that the duration of the first rest block was 25 sec (20-sec x 16 blocks + 25 sec block = 345 sec, 138 volumes for each run). Task blocks for each of the four Self conditions (two levels of feedback timing x two levels of action kinematics) were repeated twice in each Self run, while those for each of the four Other conditions were repeated twice in each Other

run (2 reps/run x 4 runs = 8 repetitions for each condition). The order of task conditions within each run was pseudo-randomized. The order of the Self and Other runs was counter-balanced across participants.

### 2.4. Stimulus presentation

In order to allow presentation of participant actions in real-time during the Self/No-delay/Concordant (SNC) condition and in video-clips in the remaining seven conditions, a screen splitter was connected to a video camera (SONY Handycam; Sony, Tokyo, Japan), personal computer, and projector (DLA-M200L; Victor, Yokohama, Japan). The experimenter manually switched the screen splitter to present either real-time actions or video clips. These video clips and auditory cues were presented using Presentation software (version 14.7, Neurobehavioral Systems, Inc., CA, USA) (Fig. 2a). In all conditions, the participants observed actions from the palm side of the hands (i.e., as if seeing a reflection in the mirror), and they were not able to see other body parts.

### 2.5. Stimulus preparation

We created video clips of each condition except for that in which real-time feedback was provided for self-actions. Each 20-sec video clip consisted of five finger gestures performed in succession by either the participant (Self conditions) or the experimenter (ATS; Other conditions). Video clips were created as follows:

Participants underwent video recording of finger gestures on a separate day from the fMRI experiment. In order to record finger actions as if they were actually performed during the experiment, participants lay on the MR scanner and extended their right forearms such that their palms were located at the center of the recorded video (Fig. 2b). A black cloth was set as the background. A digital video camera (HDC-TM350, Panasonic corp., Osaka, Japan), which was positioned outside of the MRI scanner room, recorded the finger gestures. Participants made eight sequences of finger gestures using their right hand, each of which consisted of five finger gestures for 20 sec. Each of the five finger gestures represented a single number between 1 and 5 (Fig. 1b). The order of the gestures in each sequence was randomized. The movies for the Other conditions were recorded in the same manner. The video-clips were edited such that each finger gesture was performed exactly at 2, 6, 10, 14, and 18 sec from the onset of the video clip. In total, we prepared 24 and 32 video clips for the Self and Other conditions, respectively.

### 2.6. Task conditions

The setup of the main experiment was the same as that used during the video recording session, except that each participant held a response button in his/her left hand. During the task block, participants executed finger gestures in response to auditory cues and observed visual feedback. To maintain the participant's attention to the relationship between executed actions and their visual feedback, they were instructed to judge the degree of contingency. A yellow cross was presented for 2 sec in the subsequent rest block (Fig. 1c).

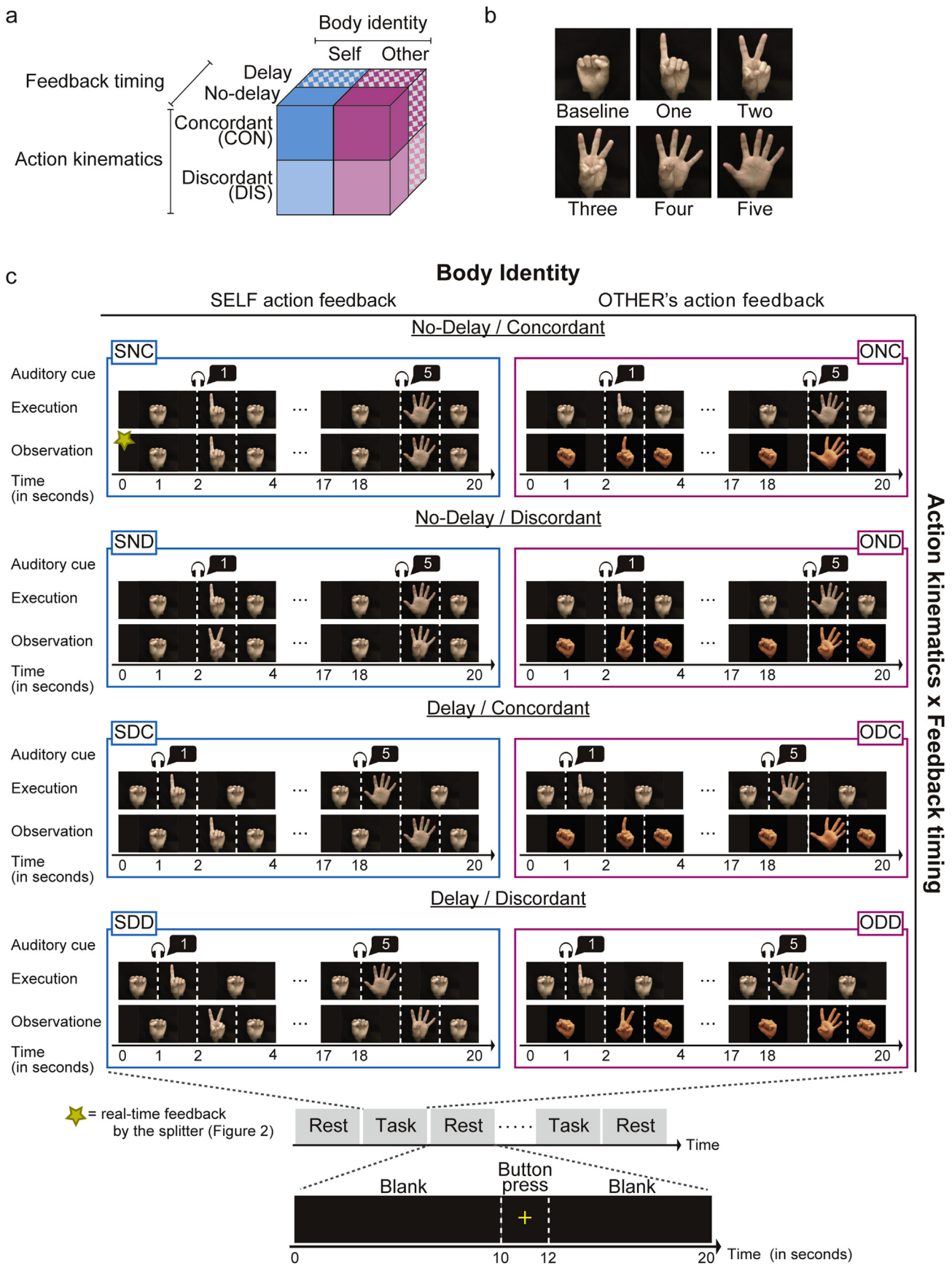


**Fig. 1 – Task conditions and procedure. (a) The experimental conditions were defined based on the manipulation of three factors: body identity (self or other), feedback timing (no-delay or delay), and action kinematics (concordant or discordant).**

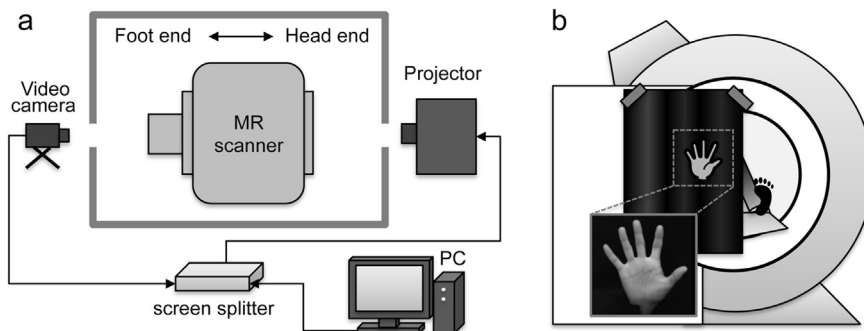


**Fig. 2 – Experiment setup. (a) Video camera settings during the fMRI experiment: During fMRI scanning, a digital video camera was positioned outside the scanner at the foot end, approximately 4 m from the participants' hands. Recorded images and visual stimuli were presented using a projector, which was controlled by a personal computer. Projected images were controlled by switching the output channel of the screen splitter. (b) A schematic view from outside of the MR scanner. A magnified window shows an actual image captured by the video camera. Video clips of these magnified images were used as visual stimuli.**

Once the cross was presented, the participant pressed one of the three buttons to rate the degree of contingency at three levels in terms of kinematics and movement onset (1 for weak contingency and 3 for strong contingency). Auditory cues and video clips were presented under eight conditions (Fig. 1c).

#### 2.6.1. Self/No-Delay/Concordant (SNC) and Other/No-Delay/Concordant (ONC) conditions

In the SNC condition, participants observed their own finger movements in real-time (Figs. 1c and 2a). Participants were instructed to execute finger gestures immediately following auditory cues presented 2, 6, 10, 14, and 18 sec after the onset of each block. We assumed that the participant would experience perfect contingency in this condition. The ONC condition was identical to the SNC condition in that participants observed gestures in the appropriate order at the time of execution. However, participants viewed clips of finger gestures performed by the experimenter. Auditory cues and gestures were presented at the same time in the ONC condition.

#### 2.6.2. Self/No-Delay/Discordant (SND) and Other/No-Delay/Discordant (OND) conditions

As in the SNC condition, in the SND condition participants observed their own finger movements at the time of action execution. However, the executed and observed gestures were not identical (Fig. 1c). Auditory cues were presented at the same timing as in the SNC and ONC conditions. Video clips depicting a sequence of finger gestures that differed from the order in which the gestures were executed were presented. The OND condition was identical to the SND condition, except that the experimenter performed the action.

#### 2.6.3. Self/Delay/Concordant (SDC) and Other/Delay/Concordant (ODC) conditions

In the SDC condition, participants viewed clips in which their own finger gestures were presented in the order of execution. However, unlike in the SNC and SND conditions, participants observed the finger gesture 1 sec after execution of the finger gesture: auditory cues were presented 1, 5, 9, 13, and 17 sec after the onset of each block, whereas gestures in each video clip were presented at 2, 6, 10, 15, and 18 sec (Fig. 1c). The ODC condition was identical to the SDC condition, except that the experimenter performed the action. We assumed that the ODC condition corresponded to being imitated by another person.

#### 2.6.4. Self/Delay/Discordant (SDD) and Other/Delay/Discordant (ODD) conditions

As in the SDC condition, participants viewed clips of their own finger gestures 1 sec after execution of the movement in the SDD condition. However, unlike in the SDC condition, the executed and observed gestures were not identical (Fig. 1c). The ODD condition was identical to the SDD condition, except that the experimenter performed the action.

### 2.7. Data analysis

Image processing and statistical analyses of fMRI data were performed using the Statistical Parametric Mapping (SPM8) package (Friston, Ashburner, Kiebel, Nichols, & Penny, 2011). The first six volumes of each run were discarded and the remaining volumes were used for analysis. After spatial realignment and slice-timing correction, all functional images

**(b) Finger gestures used in the experiment. The participants used their right hands to perform figure gestures. (c) A block design was used. During the task period, participants executed finger gestures according to and immediately after auditory instruction, following which visual feedback was provided. During the rest period after the task, participants rated the similarity of executed and observed actions upon presentation of a yellow cross. Note that the participant observed his or her own actions in real-time during the Self/No-delay/Concordant condition using the setup shown in Fig. 2. In the remaining conditions, participants viewed clips that had been recorded prior to the experiment. ODC: Other/Delay/Concordant; ODD: Other/Delay/Discordant; ONC: Other/No-Delay/Concordant; OND: Other/No-Delay/Discordant; SDC: Self/Delay/Concordant; SDD: Self/Delay/Discordant; SNC: Self/No-Delay/Concordant; SND: Self/No-Delay/Discordant.**

were co-registered to the corresponding T1 anatomical image of each participant, following which they were normalized to a T1 template in Montreal Neurological Institute space (MNI; Friston et al., 2011). The spatially normalized images were filtered using a Gaussian kernel of 8 mm full-width at half maximum (FWHM) in the x-, y-, and z-axes.

We conducted a classical mass-univariate analysis using a general linear model (Friston et al., 2011). The BOLD signal for all the tasks was modeled with boxcar functions convolved with the canonical hemodynamic response function. Each run in the design matrix included eight regressors for the task conditions and one regressor for the timing of the button press. We also added six regressors that represented motion correction parameters. The time series for each voxel was high-pass filtered at 1/128 Hz. Serial autocorrelation of the fMRI time series was corrected using a first-order autoregressive {AR (1)} model. Contrast images from the individual analyses were used for the group analysis, with between-subjects variance modeled as a random factor. We conducted a whole-brain analysis followed by a region-of-interest (ROI) analysis using one-sample t tests.

### 2.7.1. Whole-brain analysis

We initially evaluated brain regions whose activity was influenced by interactions among action kinematics, feedback timing, and body identity (Table 1). We then evaluated the main effects of each factor. We also compared the SNC/ODC conditions (corresponding to perfect contingency/being imitated) to other conditions in order to more directly examine regions sensitive to SNC and ODC. The resulting set for each contrast constituted the SPM {t}. The statistical threshold for the spatial extent test on the clusters was set at  $p < .05$ , family-wise error (FWE) corrected for multiple comparisons over the whole brain, with a height threshold of SPM {t} > 3.48, corresponding to an uncorrected  $p < .001$  (Flandin & Friston, 2017). The anatomical locations of activated regions were defined and labeled in accordance with probabilistic atlases (Eickhoff et al., 2005; Shattuck et al., 2008).

### 2.7.2. Region of interest (ROI) analysis

We originally hypothesized that three-way interactions would be observed in the LPFC and EBA. To further evaluate this hypothesis, we conducted an ROI analysis within these two regions. The statistical threshold was the same as that utilized for the whole-brain analysis, except that the search volume was limited to each area as follows.

**2.7.2.1. LATERAL PREFRONTAL CORTEX.** We combined the superior, middle, and inferior frontal gyrus in the anatomical map (Shattuck et al., 2008). To remove the medial prefrontal cortex from the ROI, regions with y coordinates less than -20 or greater than 20 were included in the search volume (82,328 mm<sup>3</sup> for the left hemisphere; 93,216 mm<sup>3</sup> for the right hemisphere) (Takahashi et al., 2015; Van Overwalle, 2009).

**2.7.2.2. EBA.** Previously, we observed that a portion of the EBA is more sensitive to imitated actions than to non-imitated actions (Okamoto et al., 2014). Using the same MRI scanner utilized during the main experiment of the present study, we

repeated the experiments of Okamoto et al. (2014) (functional localizer experiments). Eighteen healthy participants who had not participated in the main experiment were recruited. We first localized the EBA, which was more strongly activated when participants viewed non-face body parts than other objects (e.g., face, body, scene, car). We then evaluated areas within the EBA that exhibited stronger activation during concordant conditions than during discordant conditions. These areas within EBA were defined as ROIs (see Supplementary Methods and Results for details). The statistical threshold was identical to that utilized in the main experiment.

### 2.7.3. Effective connectivity analysis

We conducted effective connectivity analysis using dynamic causal modeling (DCM) (DCM12) (Friston, Harrison, & Penny, 2003). DCM is used to compare different hypotheses about the mechanisms in terms of neuronal coupling that underlie regional responses detected in conventional activity analyses (Stephan et al., 2010). This approach does not involve circularity (or double dipping), as the mass-univariate analysis of brain activation does not test any interregional relationship (Stephan et al., 2010), and hence has been used in other studies (e.g., Heim et al., 2009; Matsuyoshi et al., 2015; Sasaki, Kochiyama, Sugiura, Tanabe, & Sadato, 2012; Werner & Noppeney, 2010).

Our question was whether the EBA was involved as a node of the network accounting for the three-way interaction in the left IFG/MFG. We chose the left SPL and left EBA for two reasons. First, these regions are considered to be nodes of the brain networks involved in both action execution and observation (Caspers et al., 2010; Gazzola & Keysers, 2009; Okamoto et al., 2014). Second, activity of these regions showed either main effects or interactions of the three factors in the same hemisphere. We also defined the occipital pole (OP) as a node that receives visual input to drive the models (Sasaki et al., 2012).

In order to explain the three-way interaction in the IFG/MFG, it is necessary to identify modulation of connectivity from the OP by the three factors (see Tettamanti et al., 2008; Heim et al., 2009; Sasaki et al., 2012 for the same approach). As activity in the left EBA showed a main effect of action kinematics, it was assumed that connectivity from the OP to EBA was modulated by the effect of action kinematics. We then tested if connectivity from the EBA to IFG/MFG was modulated by a body identity × feedback timing interaction. Likewise, as the SPL showed a body identity × feedback timing interaction, we assumed that connectivity from the OP to SPL was modulated by the same interaction and tested if the connectivity from the SPL to IFG/MFG was modulated by action kinematics.

Preprocessing of fMRI data was the same as the brain activation analysis, except that we used a finer smoothing kernel (4-mm FWHM Gaussian kernel) to increase the regional specificity. Functional images from eight separate runs were concatenated as a single run to form a single time series. A new design matrix modeled seven effects of the contingency detection task in the form of parametric modulation on visual stimulation (three main effects, three two-way interactions, and one three-way interaction), button response, and effects

**Table 1 – Predefined contrasts.**

Body identity Feedback timing Action kinematics Condition abbreviations	Self				Other			
	No-delay		Delay		No-delay		Delay	
	Con	Dis	Con	Dis	Con	Dis	Con	Dis
	SNC	SND	SDC	SDD	ONC	OND	ODC	ODD
<b>Brain regions showing three-way interactions</b>								
Body identity × Feedback timing × Action kinematics	1	-1	-1	1	-1	1	1	-1
	-1	1	1	-1	1	-1	-1	1
<b>Brain regions showing two-way interactions</b>								
Body identity × Feedback timing	-1	-1	1	1	1	1	-1	-1
	1	1	-1	-1	-1	-1	1	1
Body identity × Action kinematics	1	-1	1	-1	-1	1	-1	1
	-1	1	-1	1	1	-1	1	-1
Action kinematics × Feedback timing	1	-1	-1	1	1	-1	-1	1
	-1	1	1	-1	-1	1	1	-1
<b>Brain regions showing main effects</b>								
Action kinematics	1	-1	1	-1	1	-1	1	-1
	-1	1	-1	1	-1	1	-1	1
Body identity	1	1	1	1	-1	-1	-1	-1
	-1	-1	-1	-1	1	1	1	1
Feedback timing	1	1	-1	-1	1	1	-1	-1
	-1	-1	1	1	-1	-1	1	1
<b>Brain regions more sensitive to perfect contingency (SNC) and being imitated (ODC)</b>								
SNC and ODC	3	-1	-1	-1	-1	-1	3	-1
	-3	1	1	1	1	1	-3	1
<b>Direct comparison between perfect contingency (SNC) and being imitated (ODC)</b>								
SNC versus ODC	3	-1	-1	-1	1	1	-3	1
	-3	1	1	1	-1	-1	3	-1

Con: concordant; Dis: discordant.

of no interest (six run effects and six realignment parameters) (Stephan et al., 2010). We used the same high-pass filter and AR model as in the brain-activation analysis.

The coordinates of the ROI centers were defined by the local maximum voxel in the group analysis that showed a positive average effect for all conditions for the OP; a main effect of action kinematics for the EBA; a two-way interaction (body identity × feedback timing) for the SPL; and a three-way interaction for the IFG/MFG. The ROI time-series data for each participant were extracted from voxels within a 4-mm radius centered on the predefined ROI coordinates. The data were adjusted for effects of no interest, high-pass filtered, and corrected for serial correlation.

We assumed baseline connectivity between all nodes except for the direct connections between the OP and IFG/MFG (Fig. 7). A driving input of visual stimuli was given to the OP in all models. As explained above, we used action kinematics and 2-way interaction of body identity × feedback timing as modulators. All models assumed that the connectivity from the OP to EBA was modulated by action kinematics and that the connectivity from the OP to SPL was modulated by the body identity × feedback timing interaction. We manipulated the presence of modulatory effects on the connectivity to the IFG/MFG from the EBA and SPL. There are four possibilities for each connectivity to the IFG/MFG: two modulations (action kinematics or body identity × feedback timing interaction), single modulations, or no modulation. Thus, we compared 16 DCM models.

We then performed random-effects Bayesian model selection (BMS), in which the model of each participant was

treated as a random variable, and the parameters of a Dirichlet distribution, which describes the probabilities for all models, were estimated. These probabilities define a multinomial distribution over model space, which allows us to compute the exceedance probability of one model being more likely than any other model (Stephan, Penny, Daunizeau, Moran, & Friston, 2009). We conducted BMS at both the family level and the model level (Penny et al., 2010). We separated the 16 models into four model families based on (1) modulation of action kinematics (on both connections from the EBA to the IFG/MFG and from the SPL to the IFG/MFG; on either one of them; or none) and (2) modulation of the 2-way interaction effect (body identity × feedback timing). In the model level inference, the 16 models were compared without any family definitions. After the best family and model was inferred, we evaluated the parameter estimates of connectivity in the best model with one-sample *t*-tests.

### 3. Results

#### 3.1. Behavioral results

Table 2 shows the average ratings of perceived contingency between executed and observed actions. As expected, the degree of contingency was greater for concordant conditions than for discordant conditions and greater for No-Delay conditions than Delay conditions. A repeated-measures ANOVA with three factors (body identity × feedback timing × action kinematics) revealed significant main effects of timing ( $F_{(1, 130)}$

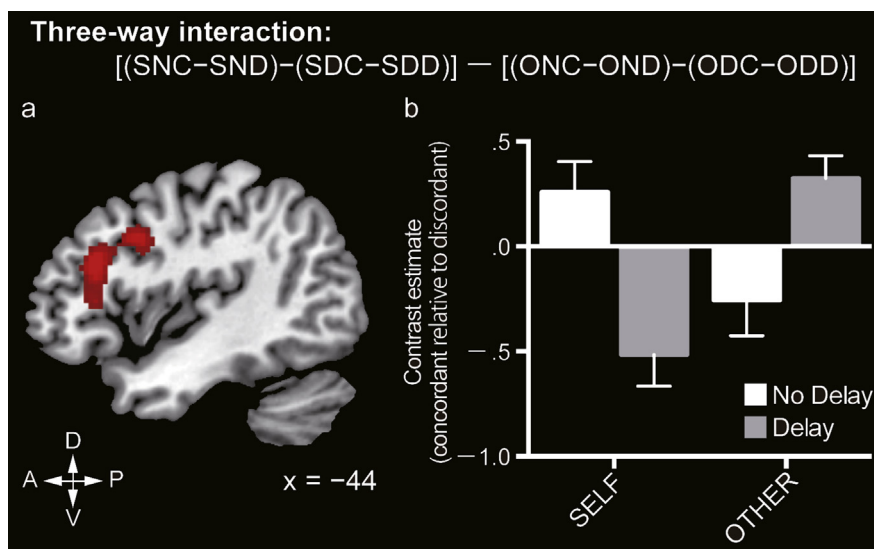


**Fig. 3 – Three-way interactions (whole-brain analysis).** (a) A three-way interaction was observed for the contrast of  $[(\text{SNC} - \text{SND}) - (\text{SDC} - \text{SDD})] - [(\text{ONC} - \text{OND}) - (\text{ODC} - \text{ODD})]$ . Areas exhibiting significant activation are shown in red on a sagittal section of a representative brain. The threshold was set at  $p < .05$ , FWE corrected for multiple comparisons at the cluster level over the whole-brain, with the height threshold of  $p < .001$  uncorrected. (b) The graph indicates the contrast estimate of concordant conditions relative to that of discordant conditions, averaged within the activated cluster. All error bars indicate the standard error of mean. A, anterior; D, dorsal; P, posterior; V, ventral. Three-way repeated-measures ANOVA on the contrast estimates confirmed a significant three-way interaction ( $F_{(1, 23)} = 36.996, p < .001$ ). Post-hoc pairwise comparisons (with Bonferroni correction) revealed that the effect of concordance (i.e., activity during the concordant condition relative to the discordant condition) was significantly greater in the Self/No-Delay condition than in the Self/Delay and the Other/No-Delay conditions ( $p = .002$  and  $.022$ , respectively). The same concordance effect was significantly greater in the Other/Delay condition than in the Self/Delay and the Other/No-Delay conditions ( $p < .001$  and  $= .003$ , respectively). ODC: Other/Delay/Concordant; ODD: Other/Delay/Discordant; ONC: Other/No-Delay/Concordant; OND: Other/No-Delay/Discordant; SDC: Self/Delay/Concordant; SDD: Self/Delay/Discordant; SNC: Self/No-Delay/Concordant; SND: Self/No-Delay/Discordant; FWE: family-wise error; ANOVA: analysis of variance.

$_{23} = 9.04, p = .006$ ) and action kinematics ( $F_{(1, 23)} = 32.89, p < .001$ ). We also observed a significant two-way interaction between body identity and action kinematics ( $F_{(1, 23)} = 5.15, p = .033$ ), with a stronger effect of concordance (Concordant > Discordant condition) for Other conditions than Self conditions. Collectively, these findings indicate that participants attended to the relationship between executed and observed actions.

### 3.2. Brain activation analysis

We initially evaluated the interactions and main effects of body identity, feedback timing, and action kinematics. We then focused on brain areas associated with both perfect contingency and being imitated.

#### 3.2.1. Three-way interaction effects (body identity $\times$ feedback timing $\times$ action kinematics)

A contrast of three-way interaction effects  $\{[(\text{SNC} - \text{SND}) - (\text{SDC} - \text{SDD})] - [(\text{ONC} - \text{OND}) - (\text{ODC} - \text{ODD})]\}$  revealed significant activation in the left inferior frontal gyrus (IFG) and middle frontal gyrus (MFG) in the whole-brain analysis (Fig. 3, Table 3). Activation in the left IFG and MFG overlapped with the ROI of the left LPFC. We observed no additional significant activation when the search volume was limited to each ROI. As this activation was induced by both the

effect of self-agency  $[(\text{SNC} - \text{SND}) - (\text{SDC} - \text{SDD})]$  and the effect of social contingency  $[(\text{ODC} - \text{ODD}) - (\text{ONC} - \text{OND})]$ , we conducted a supplementary analysis to compare them. However, no significant activation was revealed, regardless of whether the whole brain or ROI analysis was used.

No significant activation was observed for the opposite contrast  $\{[(\text{ONC} - \text{OND}) - (\text{ODC} - \text{ODD})] - [(\text{SNC} - \text{SND}) - (\text{SDC} - \text{SDD})]\}$ .

#### 3.2.2. Two-way interactions

In the whole-brain analysis, a contrast of body identity  $\times$  feedback timing interactions  $\{[(\text{ONC} + \text{OND}) - (\text{ODC} + \text{ODD})] - [(\text{SNC} + \text{SND}) - (\text{SDC} + \text{SDD})]\}$  revealed significant activation in the bilateral SPL, right precentral gyrus (PreCG), right inferior/middle temporal gurus (ITG/MTG), and left postcentral gyrus (PostCG) (Table 4 and Fig. 4). The activation in the right ITG/MTG overlapped with the ROI for the right EBA. No additional significant activation was observed in the ROI analysis. The opposite contrast  $\{[(\text{SNC} + \text{SND}) - (\text{SDC} + \text{SDD})] - [(\text{ONC} + \text{OND}) - (\text{ODC} + \text{ODD})]\}$  revealed no significant activation.

We then evaluated body identity  $\times$  action kinematics interactions. The whole brain analysis revealed no significant activation. In the ROI analysis, the contrast of  $\{[(\text{SNC} - \text{SND}) + (\text{SDC} - \text{SDD})] - [(\text{ONC} - \text{OND}) + (\text{ODC} - \text{ODD})]\}$  revealed significant activation in the right superior frontal

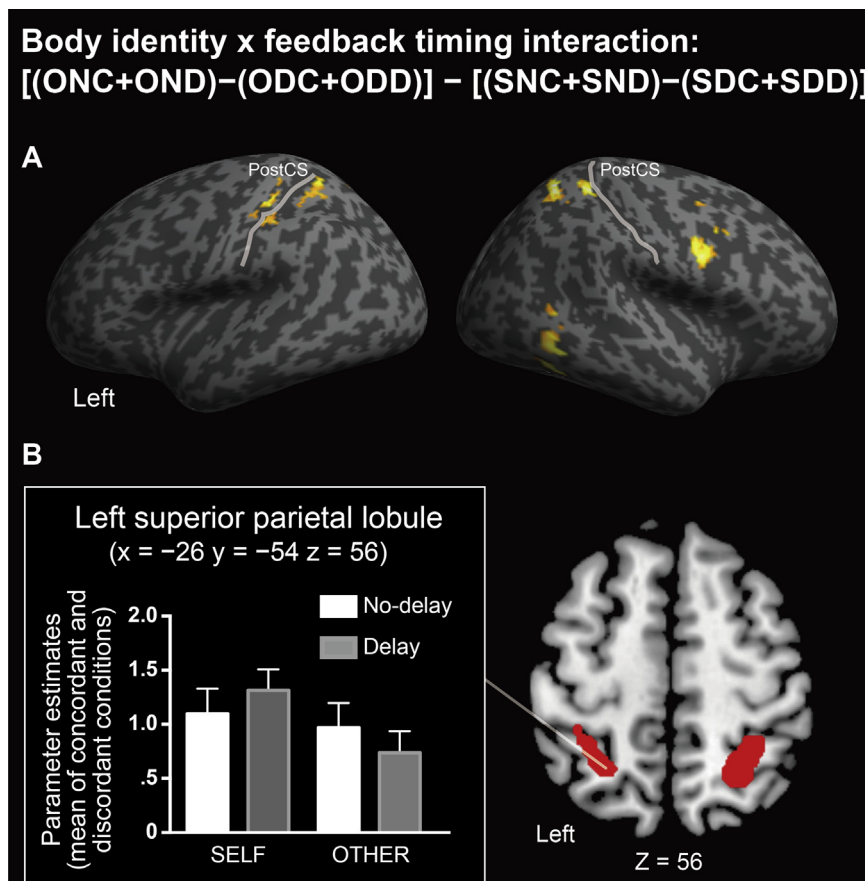


**Fig. 4 – Body identity and feedback timing interaction. Brain regions showing body identity and feedback timing interaction depicted by the contrast of  $[(ONC + OND) - (ODC + ODD)] - [(SNC + SND) - (SDC + SDD)]$ . Activated regions are shown on (a) the surface-rendered MRI of a representative brain and (b) a horizontal section. The threshold was set at  $p < .05$ , FWE corrected for multiple comparisons at the cluster level over the whole-brain, with the height threshold of  $p < .001$  uncorrected. Three-way repeated-measures ANOVA on the contrast estimates at peak coordinates of the superior parietal lobule confirmed a significant two-way interaction of body identity and feedback timing ( $F_{(1, 23)} = 15.904, p < .001$ ) and main effect of body identity. PostCS: Postcentral sulcus; ODC: Other/Delay/Concordant; ODD: Other/Delay/Discordant; ONC: Other/No-Delay/Concordant; OND: Other/No-Delay/Discordant; SDC: Self/Delay/Concordant; SDD: Self/Delay/Discordant; SNC: Self/No-Delay/Concordant; SND: Self/No-Delay/Discordant; FWE: family-wise error.**

gyrus (SFG) of the LPFC (Table 4). No significant activation was observed for the opposite contrast  $\{[(ONC - OND) + (ODC - ODD)] - [(SNC - SND) + (SDC - SDD)]\}$ .

Finally, we evaluated the contrasts of action kinematics  $\times$  feedback timing interactions. The whole brain analysis revealed no significant activation. In the ROI analysis, the contrast of  $\{[(SDC - SDD) - (SNC - SND)] + [(ODC - ODD) - (ONC - OND)]\}$  revealed a significant activation in the ITG within the right EBA (Table 4).

### 3.2.3. Main effects

We first evaluated the main effect of action kinematics. The contrast of  $[(SNC + SDC + ONC + ODC) - (SND + SDD + OND + ODD)]$  revealed no significant activation in the whole-brain analysis. In the ROI analysis, the same contrast revealed significant activation in the bilateral EBA (Fig. 5). The opposite contrast of  $[(SND + SDD + OND + ODD) - (SNC + SDC + ONC + ODC)]$  revealed significant activation in the right superior occipital gyrus, right cuneus, and left

cuneus/SPL (Table 5). No additional activation was observed in the ROI analysis.

Next, we evaluated the main effects of body identity. The contrast of  $[(SNC + SND + SDC + SDD) - (ONC + OND + ODC + ODD)]$  revealed significant activation in the right PostCG and SPL. The opposite contrast of  $[(ONC + OND + ODC + ODD) - (SNC + SND + SDC + SDD)]$  revealed significant activation in the medial portion of the left SFG (Table 5). ROI analysis revealed no additional activation. Finally, neither whole-brain nor ROI analysis for the main effect of feedback timing revealed significant activation.

### 3.2.4. Perfect contingency (SNC) and being imitated (ODC)

We examined differences between conditions associated with perfect contingency and being imitated. The contrast of perfect contingency (SNC) against being imitated (ODC) revealed significant activation in the right SPL and inferior parietal lobule (IPL) (Table 6). The opposite contrast revealed no significant activation. No additional activation was identified in the ROI analysis.

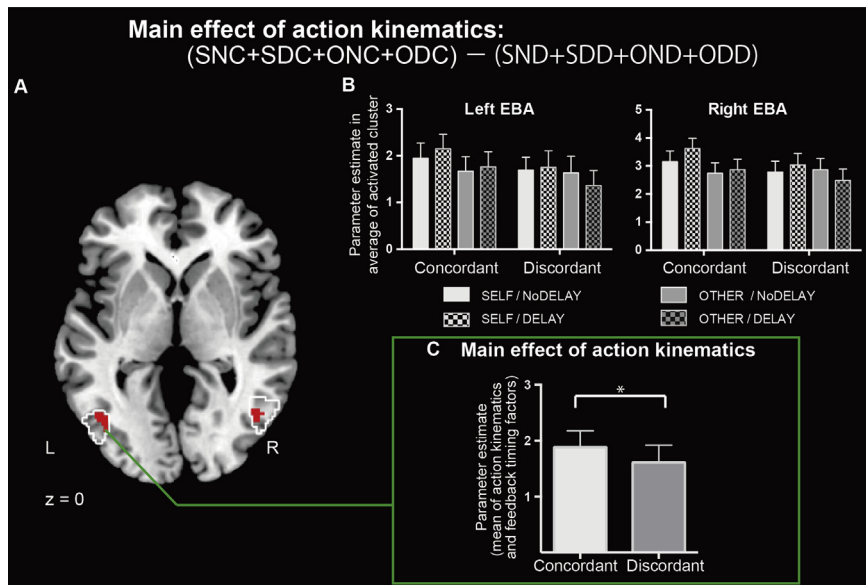


**Fig. 5 – The main effect of action kinematics. (a)** A significant effect of action kinematics was observed by the contrast of [(SNC + SDC + ONC + ODC) – (SND + SDD + OND + ODD)]. Areas exhibiting significant activation are shown in red on a horizontal section of a representative brain. We limited our search volume to the EBA based on the results of an independent localizer task (indicated by white lines, see [Supplemental Information for details regarding ROI selection](#)). The threshold was set at  $p < .05$ , FWE corrected for multiple comparisons at the cluster level over the whole-brain, with the height threshold of  $p < .001$  uncorrected. **(b)** The graph indicates the value of the parameter estimate, averaged within each cluster. Three-way ANOVA (Body identity  $\times$  Feedback timing  $\times$  Action kinematics) on the left EBA revealed a significant main effect of action kinematics [ $F(1,23) = 14.99, p = .001$ ] and main effect of body identity [ $F(1,23) = 4.57, p = .043$ ]. The same ANOVA on the right ROI revealed a significant main effect of action kinematics [ $F(1,23) = 13.18, p = .001$ ], and interaction of body identity and feedback timing [ $F(1,23) = 14.87, p < .001$ ]. **(c)** The graph indicates the averaged parameter estimates for the concordant and discordant conditions in the left EBA. All error bars indicate standard error of mean. L, left; R, right. \*,  $p < .05$ . ODC: Other/Delay/Concordant; ODD: Other/Delay/Discordant; ONC: Other/No-Delay/Concordant; OND: Other/No-Delay/Discordant; SDC: Self/Delay/Concordant; SDD: Self/Delay/Discordant; SNC: Self/No-Delay/Concordant; SND: Self/No-Delay/Discordant; FWE: family-wise error; ANOVA: analysis of variance; EBA: extrastriate body area.

We then investigated which brain regions were more active in the SNC and ODC conditions than in other conditions. As we observed no significant differences other than those in the SPL and IPL, we evaluated the SNC and ODC conditions against the remaining conditions (SNC + ODC vs others). While whole-brain analysis revealed no significant activation, ROI analysis revealed activation in the left MFG and IFG (Fig. 6, Table 6), which overlapped with the region activated by the three-way interaction (Fig. 6).

Collectively, our analyses revealed a three-way interaction in the left IFG and MFG, two-way interactions in multiple brain regions including a body identity  $\times$  feedback timing interaction in the bilateral SPL, and a concordance effect on action kinematics within the bilateral EBA. The IFG/MFG showed stronger activation in SNC and ODC than other conditions. While significant two-way interactions were observed in the right EBA (body identity  $\times$  feedback timing; action kinematics  $\times$  feedback timing), no such interaction effects were observed in the left EBA.

### 3.3. Effective connectivity analysis

We conducted a DCM analysis to model the relationship between the IFG/MFG and other regions (Fig. 7). We focused our

analysis on the left hemisphere given that the left IFG/MFG showed a three-way interaction. We chose the other nodes based on the following two criteria: (1) they were considered as parts of the brain networks involved in both action execution and observation (Gazzola & Keysers, 2009); (2) they showed either a main effect or an interaction effect in the brain activation analysis. Consequently, the left EBA and SPL were chosen as nodes in this analysis. We added the OP as a region receiving visual input. The main hypothesis was that connectivity from the OP to the IFG/MFG (via either the EBA or SPL) is modulated by the factors to induce the three-way interactions in the IFG/MFG: modulation by action kinematics of the connectivity from the SPL to the IFG/MFG or modulation by feedback timing and identity of the connectivity from the EBA to the IFG/MFG (Fig. 7A). We compared the 16 models that assumed different types of modulations of the connections from the EBA or SPL to the IFG/MFG (Fig. 7B).

We performed two analyses assuming different model families (one categorized by the effects of action kinematics and the other categorized by the effects of 2-way interaction (body identity  $\times$  feedback timing) (Fig. 7B). In the former analysis, the highest exceedance probability was obtained in the model family that assumed modulatory effects of action

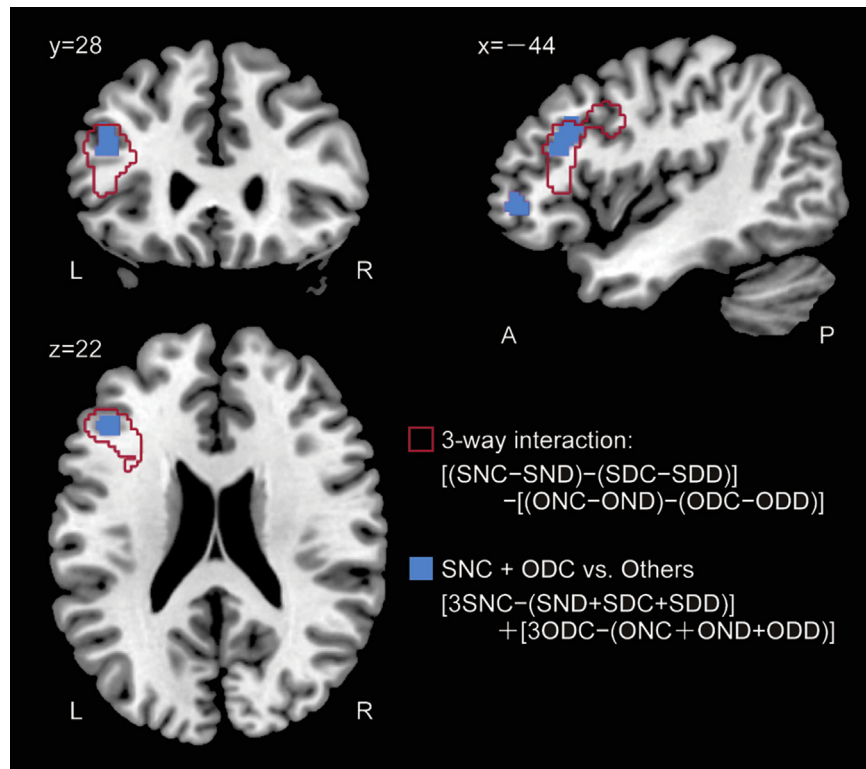


**Fig. 6 – Greater activation in SNC and ODC than the other conditions.** Brain activation in the SNC and ODC conditions relative to other conditions was depicted by the contrast of  $[3\text{SNC} - (\text{SND} + \text{SDC} + \text{SDD})] + [3\text{ODC} - (\text{ONC} + \text{OND} + \text{ODD})]$  (indicated in cyan). The threshold was set at  $p < .05$ , FWE corrected for multiple comparisons at the cluster level over the lateral prefrontal cortex (small volume correction), with the height threshold of  $p < .001$  uncorrected. Regions outlined in red indicate areas in which three-way interactions were observed (i.e., corresponding with Fig. 3). A, anterior; L, left; P, posterior; R, right; ODC: Other/Delay/Concordant; ODD: Other/Delay/Discordant; ONC: Other/No-Delay/Concordant; OND: Other/No-Delay/Discordant; SDC: Self/Delay/Concordant; SDD: Self/Delay/Discordant; SNC: Self/No-Delay/Concordant; SND: Self/No-Delay/Discordant; FWE: family-wise error.

kinematics on both connectivity from the EBA to the IFG/MFG and from the SPL to the IFG/MFG (Fig. 7 C1). The other model family analysis showed that the exceedance probability was the highest in the model family that assumed no modulatory effect of the 2-way interaction (body identity  $\times$  feedback timing) on these two connections (Fig. 7 C2). Finally, at the level of model inference, the exceedance probability was the highest in Model 4 (42.1%) in which the factor of action kinematics had a modulatory effect on connections from the SPL and EBA to the IFG/MFG (Fig. 7 C3).

One-sample  $t$  tests on parameter estimates showed that intrinsic connectivity from the OP to EBA and from the OP to SPL, as well as the driving input to the OP were significantly greater than zero ( $p$  values  $< .05$ , false-discovery rate corrected) (Supplemental Table 3). However, no other intrinsic connectivity or modulatory effect showed significant effect.

#### 4. Discussion

In the present study, we identified a distributed set of brain regions sensitive to body identity, feedback timing, and action kinematics during the evaluation of contingency between

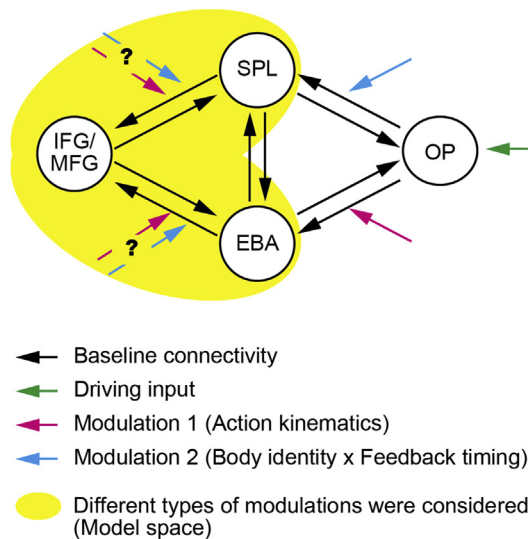
executed and observed actions. Three-way interactions of these factors were observed in the left IFG and MFG. Stronger effects of concordance in action kinematics were observed in these regions both when real-time feedback was presented for self-actions (Self/No-delay) and during the presentation of imitated actions (Other/Delay), relative to those observed in other conditions (Fig. 6). In contrast, main effects of action kinematics were observed in the left EBA.

##### 4.1. Three-way interactions in the IFG and MFG

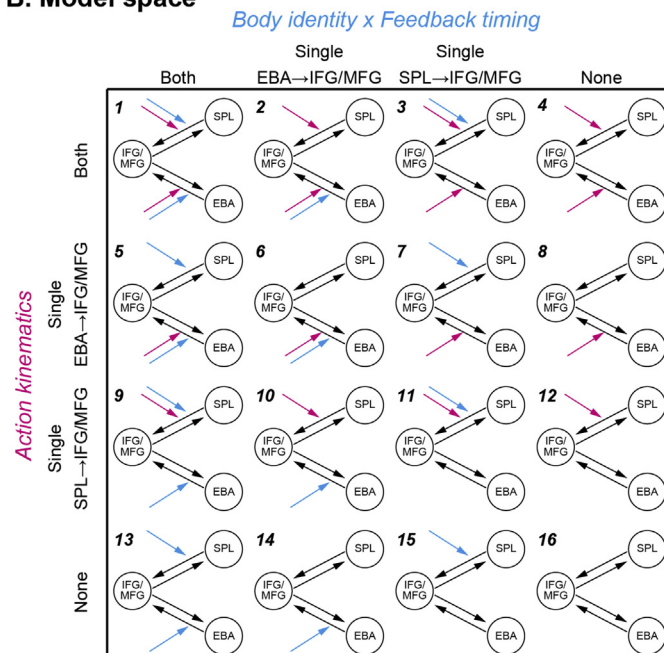
To the best of our knowledge, the present study is the first to demonstrate interaction effects among action kinematics, body identity, and feedback timing in the IFG and MFG during the observation of actions contingent on one's own actions. These regions were more sensitive to perfect contingency (SNC) and being imitated (ODC) than to other conditions, suggesting that the IFG and MFG are involved in the integration of contingency signals when detecting perfect and less-than-perfect contingency.

Previous studies have demonstrated the role of the IFG and MFG in identifying imitated actions (Decety et al., 2002; Guionnet et al., 2012) and in shaping the sense of agency (Fukushima, Goto, Q5

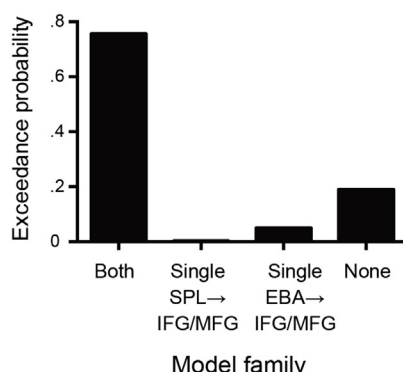
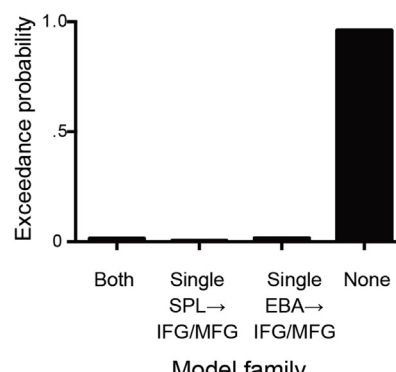
## A. Basic model for model construction



## B. Model space



## C. Results of Bayesian Model Selection

C1. Family level inference  
(Action kinematics)C2. Family level inference  
(Body identity x Feedback timing)

## C3. Model level inference

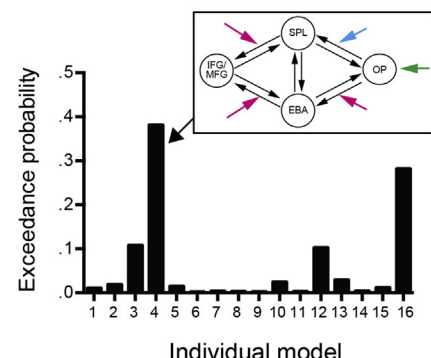


**Fig. 7 – Dynamic causal modeling (DCM) analysis. (A)** DCM models were based on four ROIs: Occipital pole (OP), EBA, superior parietal lobule (SPL), and IFG/MFG. All models had identical baseline connections (black arrows) and driving input to OP (green arrow). Based on brain activation analysis, we assumed modulations by action kinematics of the connectivity from OP to EBA (magenta arrow) and by a body identity  $\times$  feedback timing interaction of the connectivity from OP to SPL (cyan arrow). By manipulating the modulators of action kinematics and body identity  $\times$  feedback timing to the connectivity from EBA to IFG/MFG and that from SPL to IFG/MFG (highlighted area), we tested 16 models. The coordinates for the OP were  $(-24, -92, 6)$ . **(B)** The 16 tested models. Labels in rows indicate the model families categorized by action kinematics modulation, and those in columns indicate the model families categorized by body identity  $\times$  feedback timing modulation. **(C)** Results of Bayesian model selection (BMS).

Maeda, Kato, & Umeda, 2013; Kontaris, Wiggett, & Downing, 2009) and body ownership (Limanowski & Blankenburg, 2016; Tsakiris, Longo, & Haggard, 2010). For example, concordance between movement of an individual's own arm and observed visual feedback results in greater activation within a brain network that includes the IFG (Limanowski & Blankenburg, 2016). However, as none of these studies comprehensively examined brain activity sensitive to the body identity, feedback timing, and

action kinematics, previous evidence has been unable to demonstrate whether these regions are involved in the integration of these three factors. The present study extends the previous findings by demonstrating that the IFG and MFG are involved in such processes.

The IFG has been regarded as a node of shared representations between actions and observed outcomes (Caspers et al., 2010; Gazzola & Keysers, 2009; Iacoboni & Dapretto, 2006;

**Table 2 – Subjective ratings of perceived contingency.**

Condition	Average	SEM
Self/No-Delay/Concordant (SNC)	2.43	.11
Self/No-Delay/Discordant (SND)	1.92	.14
Self/Delay/Concordant (SDC)	2.05	.18
Self/Delay/Discordant (SDD)	1.56	.11
Other/No-Delay/Concordant (ONC)	2.48	.10
Other/No-Delay/Discordant (OND)	1.67	.13
Other/Delay/Concordant (ODC)	2.05	.18
Other/Delay/Discordant (ODD)	1.52	.12

SEM, standard error of the mean. Scores ranged from 1 (min) to 3 (max).

Molenberghs et al., 2012; Rizzolatti, Fogassi, & Gallese, 2001). Though recently challenged by several studies (e.g., Oosterhof et al., 2013; Wurm & Lingnau, 2015), the frontal node has been considered highest in the cortical hierarchy of the mirror-neuron system (MNS; Kilner, Friston, & Frith, 2007; Keysers & Gazzola, 2009). Thus, it is possible that the IFG is involved in detecting contingency between actions and outcomes at a more abstract level than other areas by integrating relevant information regarding action kinematics, feedback timing, and body identity. According to the Hebbian-learning hypothesis (Giudice, Manera, & Keysers, 2009; Keysers & Perrett, 2004), perfect contingency and being imitated may be detected in the

**Table 3 – Three-way interactions.**

Cluster	Voxel		Peak coordinate			Side	Location		
	P (FWE)	Size (mm <sup>3</sup> )	P (uncorrected)	Z-score	x			y	z
[(SNC – SND) – (SDC – SDD)] – [(ONC – OND) – (ODC – ODD)]	.001	4528	<.001	4.64	–44	28	22	L	Inferior frontal gyrus <sup>a</sup>
[(ONC – OND) – (ODC – ODD)] – [(SNC – SND) – (SDC – SDD)]			<.001	4.12	–44	10	36	L	Middle frontal gyrus
n.s.									

Anatomical location was defined and labeled in accordance with probabilistic atlases (Eickhoff et al., 2005; Shattuck et al., 2008). All *p*-values were FWE (family-wise error) corrected for multiple comparisons at the cluster level; n.s. indicates no significant activation.

<sup>a</sup> The coordinates used in the DCM analysis. ODC: Other/Delay/Concordant; ODD: Other/Delay/Discordant; ONC: Other/No-Delay/Concordant; OND: Other/No-Delay/Discordant; SDC: Self/Delay/Concordant; SDD: Self/Delay/Discordant; SNC: Self/No-Delay/Concordant; SND: Self/No-Delay/Discordant.

**Table 4 – Two-way interactions.**

Cluster	Voxel		Peak coordinate			Side	Location		
	P (FWE)	Size (mm <sup>3</sup> )	P (uncorrected)	Z-score	x			y	z
<b>Body identity × Feedback timing</b>									
[(SNC + SND) – (SDC + SDD)] – [(ONC + OND) – (ODC + ODD)]									
n.s.									
[(ONC + OND) – (ODC + ODD)] – [(SNC + SND) – (SDC + SDD)]	.033	1840	<.001	4.34	48	–52	–10	R	Inferior temporal gyrus
			<.001	3.67	54	–52	4	R	Middle temporal gyrus
.011	2408	<.001	4.33	54	8	32	R	Precentral gyrus	
.018	2160	<.001	4.13	–46	–30	46	L	Postcentral gyrus	
		<.001	3.99	–26	–54	56	L	Superior parietal lobule <sup>c</sup>	
.005	2880	<.001	4.83	26	–46	48	R	Superior parietal lobule	
<b>Body identity × Action kinematics</b>									
[(SNC – SND) + (SDC – SDD)] – [(ONC – OND) + (ODC – ODD)]	.048 <sup>a</sup>	824	<.001	3.89	18	36	50	R	Superior frontal gyrus
[(ONC – OND) + (ODC – ODD)] – [(SNC – SND) + (SDC – SDD)]									
n.s.									
<b>Action kinematics × Feedback timing</b>									
[(SNC – SND) – (SDC – SDD)] + [(ONC – OND) – (ODC – ODD)]									
n.s.									
[(SDC – SDD) – (SNC – SND)] + [(ODC – ODD) – (ONC – OND)]	.011 <sup>b</sup>	176	<.001	3.77	48	–58	–4	R	Inferior temporal gyrus

Anatomical location was defined and labeled according to probabilistic atlases (Eickhoff et al., 2005; Shattuck et al., 2008). All *p*-values were FWE (family-wise error) corrected for multiple comparisons at the cluster level; n.s. indicates no significant activation.

<sup>a</sup> The search volume for activation was limited to the lateral prefrontal cortex in each hemisphere as defined by the combination of the superior, middle, and inferior frontal gyrus in the anatomical map (Shattuck et al., 2008) for regions in which  $y < -20$  or  $y > 20$  (ROI analysis).

<sup>b</sup> The search volume for activation was limited to the EBA in each hemisphere as defined by a supplemental experiment (ROI analysis).

<sup>c</sup> The coordinates used in the DCM analysis. EBA: extrastriate body area; ROI: region of interest; ODC: Other/Delay/Concordant; ODD: Other/Delay/Discordant; ONC: Other/No-Delay/Concordant; OND: Other/No-Delay/Discordant; SDC: Self/Delay/Concordant; SDD: Self/Delay/Discordant; SNC: Self/No-Delay/Concordant; SND: Self/No-Delay/Discordant.

**Table 5 – Main effects.**

Cluster		Voxel		Peak coordinate			Side	Location
P (FWE)	Size (mm <sup>3</sup> )	P (uncorrected)	Z-score	x	y	z		
<b>Action kinematics</b>								
<b>Concordant &gt; Discordant: (SNC + SDC + ONC + ODC) – (SND + SDD + OND + ODD)</b>								
.003 <sup>b</sup>	456	<.001	4.29	46	–62	–4	R	Inferior temporal gyrus (EBA)
.006 <sup>b</sup>	288	<.001	3.78	–46	–64	0	L	Middle temporal gyrus (EBA) <sup>c</sup>
<b>Discordant &gt; Concordant: (SND + SDD + OND + ODD) – (SNC + SDC + ONC + ODC)</b>								
.001	4056	<.001	4.37	22	–68	16	R	Superior occipital gyrus
		<.001	4.24	12	–76	26	R	Cuneus
		<.001	3.62	–8	–72	26	L	Cuneus/Superior parietal lobule
<b>Body identity</b>								
<b>Self &gt; Other: (SNC + SND + SDC + SDD) – (ONC + OND + ODC + ODD)</b>								
.01	2640	<.001	4.66	62	–14	36	R	Postcentral gyrus
<.001	15,368	<.001	5.95	26	–68	38	R	Superior parietal lobule
<b>Other &gt; Self: (ONC + OND + ODC + ODD) – (SNC + SND + SDC + SDD)</b>								
.038	1896	<.001	3.8	–6	32	34	L	Superior frontal gyrus
<b>Feedback timing</b>								
<b>No Delay &gt; Delay: (SNC + SND + ONC + OND) – (SDC + SDD + ODC + ODD)</b>								
n.s.								
<b>Delay &gt; No Delay: (SDC + SDD + ODC + ODD) – (SNC + SND + ONC + OND)</b>								
n.s.								
Anatomical location was defined and labeled according to probabilistic atlases (Eickhoff et al., 2005; Shattuck et al., 2008). All p-values were FWE (family-wise error) corrected for multiple comparisons at the cluster level; n.s. indicates no significant activation.								
<sup>a</sup> The search volume for activation was limited to the lateral prefrontal cortex in each hemisphere as defined by the combination of the superior, middle, and inferior frontal gyrus in the anatomical map (Shattuck et al., 2008) for regions in which $y < -20$ or $y > 20$ (ROI analysis).								
<sup>b</sup> The search volume for activation was limited to the EBA in each hemisphere as defined by a supplemental experiment (ROI analysis).								
<sup>c</sup> The coordinate used in the DCM analysis. EBA: extrastriate body area; ROI: region of interest; ODC: Other/Delay/Concordant; ODD: Other/Delay/Discordant; ONC: Other/No-Delay/Concordant; OND: Other/No-Delay/Discordant; SDC: Self/Delay/Concordant; SDD: Self/Delay/Discordant; SNC: Self/No-Delay/Concordant; SND: Self/No-Delay/Discordant.								

**Table 6 – Perfect contingency (SNC) and being imitated (ODC).**

Cluster		Voxel		Peak coordinate			Side	Location
P (FWE)	Size (mm <sup>3</sup> )	P (uncorrected)	Z-score	x	y	z		
<b>[SNC – ODC]</b>								
.046	1672	<.001	3.79	24	–56	64	R	Superior parietal lobule
			3.38	28	–52	52	R	Inferior parietal lobule
<b>[ODC – SNC]</b>								
n.s.								
<b>SNC + ODC versus others</b>								
<b>[3SNC – (SND + SDC + SDD)] + [3ODC – (ONC + OND + ODD)]</b>								
.031 <sup>a</sup>	984	<.001	4.21	–44	28	22	L	Middle frontal gyrus
.034 <sup>a</sup>	944	<.001	4.19	–40	48	0	L	Inferior frontal gyrus
Anatomical location was defined and labeled in accordance with probabilistic atlases (Eickhoff et al., 2005; Shattuck et al., 2008). All p-values were FWE (family-wise error) corrected for multiple comparisons at the cluster level.								
<sup>a</sup> The search volume for activation was limited to the lateral prefrontal cortex in each hemisphere as defined by the combination of the superior, middle, and inferior frontal gyrus in the anatomical map (Shattuck et al., 2008) for regions in which $y < -20$ or $y > 20$ (ROI analysis). ROI: region of interest; ODC: Other/Delay/Concordant; ODD: Other/Delay/Discordant; ONC: Other/No-Delay/Concordant; OND: Other/No-Delay/Discordant; SDC: Self/Delay/Concordant; SDD: Self/Delay/Discordant; SNC: Self/No-Delay/Concordant; SND: Self/No-Delay/Discordant.								

IFG through experience in daily life. For example, when an infant raises his hand, and he concurrently views his own hand rising, simultaneous activation of the neural populations producing the motion and those that respond preferentially to the action (visual sensory neurons) occurs. After repeated execution and observation of the self-action, the motor and sensory events become coupled (Keysers & Perrett, 2004). This association process can then be applied to being imitated, when an infant raises his hand and subsequently views the hand of another person rising at a delay.

#### 4.2. Concordance effect of action kinematics in the left EBA

In contrast to findings observed in the IFG and MFG, no three-way interactions were observed in the EBA. The left EBA was sensitive to the concordance of action kinematics, but neither a main effect of feedback timing nor their interaction was observed. Two-way interactions between concordance of action kinematics and feedback timing, and between body identity and feedback timing, were observed in the right EBA,

which was also influenced by the concordance of action kinematics as a main effect.

Previous studies have revealed that the EBA is sensitive to being imitated (Chaminade, Meltzoff, & Decety, 2005; Decety et al., 2002; Okamoto et al., 2014), plays a role in identifying self-actions and developing the sense of agency (David et al., 2007; Yomogida et al., 2010), and is involved in the sense of body ownership (Limanowki et al., 2014; Limanowski & Blankenburg, 2016; Wold, Limanowski, Walter, & Blankenburg, 2014). The present study extends these findings by demonstrating that body identity and temporal delays less strongly influence the effect of concordance on activation in the EBA than in the IFG/MFG in the left hemisphere. This finding is in contrast to previous findings that highlighted the function of LOTC in representing actions at a more abstract level than the frontal regions (Oosterhof et al., 2013; Wurm & Lingnau, 2015). The participants in these studies observed other's actions without performing the same actions by themselves. Thus, it is possible that this region code observed actions at an abstract level, but code contingency between observed actions and executed actions at a simpler level.

#### 4.3. The relationship between the IFG/MFG and other regions

Our DCM analysis showed that a model with modulations of the connectivity from the SPL and EBA to the IFG/MFG by action kinematics is more likely than other models that assumed different types of modulation of the same connectivity. This result suggests that signals from the visual cortex to SPL were modulated by action kinematics, and further modulated by effects of body identity and feedback timing on the connectivity from the SPL to IFG/MFG, which results in a 3-way interaction effect in the IFG. On the other hand, signals from the early visual cortex to SPL and the SPL to IFG/MFG were modulated only by action kinematics. Thus, the EBA may contribute to the interaction in the IFG only by providing signals of congruency of action kinematics.

We previously observed a concordance effect of action kinematics in the EBA during the observation of being imitated, and proposed that this region corresponds to the CDM (Okamoto et al., 2014). In contrast, the present results suggest that the CDM is represented in distributed brain regions in a hierarchical manner, rather than within a specific brain region such as the EBA.

#### 4.4. Relationships with previous studies on the sense of agency

A previous meta-analysis study showed that a distributed network of brain regions is involved in the sense of agency (Sperduti et al., 2011). Many brain regions revealed in the present study are similar to the areas identified in that analysis, although we did not observe activation in the insula. In experimental studies, activity in the anterior part of the insula was associated with the sense of agency when body parts were used as feedback (Nahab et al., 2011; Tsakiris et al., 2010). The critical differences from these previous studies are (1) that the executed actions in the present study were more complex and varied, and (2) that additional factors (body identity and action kinematics) were

involved. These differences may lead to recruitment of a network that is activated by both action observation and execution, without the insula being associated with the marking of subjective time (Craig, 2009; Tsakiris et al., 2010).

#### 4.5. Interpretational issues and limitations

There are at least four interpretational issues and limitations. First, the participants observed their own actions online in the SNC condition, whereas they did not in the other self-conditions, such as the SDC (concordant self-actions with delay) condition, due to technical difficulties. This difference makes SNC more similar to the executed actions than SDC in detailed kinematics. However, only a negligible difference was observed in behavioral ratings (i.e., a similar difference was seen between SNC and SND and between SDC and SDD). The contingency effect in the self-delayed condition (SDC – SDD) was the opposite of the effect in the self-non-delayed condition (SNC – SND) in the IFG/MFG (Fig. 3). Thus, its effect is unlikely to explain the interaction effect of action kinematics  $\times$  feedback timing in the self-condition, which is a part of the three-way interaction in the IFG/MFG.

Second, behavioral ratings in the “other” conditions showed a stronger effect of action kinematics than in the self-conditions. It is rare in our daily life to see others performing the same actions as the participants did in this study. Thus, observation of the same actions, despite their low prior probability, may contribute to a higher rating of perceived contingency. As this effect is represented as a 2-way interaction of body identity and action kinematics, it is unlikely to explain the 3-way interaction effects in the IFG/MFG. Instead, the right superior frontal gyrus showed a 2-way interaction and hence may be associated with this behavioral effect.

Third, none of the parameter estimates for modulatory effects in the winning dynamic causal model showed significant difference from zero. This indicates that, though the IFG receives signals modulated by the manipulated factors, the patterns of excitation and inhibition are varied among the participants. As inference of model structure is done separately from inference of model parameters in the DCM analysis (Stephan et al., 2010), the selection of the model space should be sufficient to address our question. However, further research is necessary in the future about the mechanisms that explain these individual differences and how such differences affect the participants' behaviors.

Finally, we recruited a relatively small number of young participants. Broader future studies are necessary to generalize the observed effects in other populations.

#### 4.6. Directions for future research

Two future research directions are worth noting. First, our study did not examine how neural candidates for the CDM develop during early childhood. As the CDM should be more sensitive to perfect than less-than perfect contingencies, especially during early childhood (e.g., Gergely et al., 1999), future studies should investigate how developmental changes in such candidates occur. Second, future studies should examine whether dysfunction of the CDM contributes to impairments in social communication. For example, individuals

with autism spectrum disorders (ASD) exhibit atypical activation in the EBA (Okamoto et al., 2014, 2017). Congenital blindness, which can delay development of social skills (Hobson & Lee, 2010), also affects the functional organization of the EBA in adults (Kitada et al., 2014). Given that disturbance of the CDM may explain difficulties in social skills (Gergely, 2001), future studies should examine activation patterns in the neural substrates of the CDM in individuals with atypical development.

## 5. Conclusion

In the present study, we examined the neural correlates of contingency detection between executed and observed hand movements by manipulating action kinematics, body identity, and feedback timing. Three-way interactions of these factors influenced activity in the left IFG/MFG, suggesting that these regions are sensitive to agency and social contingency. In contrast, no such three-way interactions were observed in the left EBA, which was instead sensitive to the congruence of action kinematics. These results highlight the different roles of the IFG/MFG and EBA as nodes within the brain network for contingency detection. Our findings indicate that the IFG and MFG are critical for contingency detection at a level abstract enough to be selective for socially relevant contingencies. In contrast, the EBA may be involved in detecting congruence at a lower level, by processing signals associated with action kinematics.

## Author contributions

ATS, YO, RK, and NS designed the study; ATS, YO, and RK conducted the experiments; TK contributed unpublished reagents/analytic tools; ATS analyzed data; ATS, YO, and RK wrote the manuscript.

## Competing financial interests and conflicts of interest

The authors declare no competing financial interests or conflicts of interest.

## Acknowledgments

This study was supported by a Grant-in Aid for Scientific Research (S) (Grant No. 21220005; to N.S.); a Grant-in Aid for Scientific Research on Innovative Areas (Grant No. 22101001; to T.K. and N.S.) from the Ministry of Education, Culture, Sports, Science, and Technology of Japan; a start-up grant from Nanyang Technological University (to R.K.); a Grant-in-Aid for Young Scientists (B) (Grant No. 16K16585; to A.T.S and 17K17766; to Y.O.) from the Japan Society for the Promotion of Science. A portion of this study contains results associated with the “Development of biomarker candidates for social behavior” carried out under the Strategic Research Program for Brain Science by the Ministry of Education, Culture, Sports, Science, and Technology of Japan.

## Supplementary data

Supplementary data related to this article can be found at <https://doi.org/10.1016/j.cortex.2018.08.003>.

## REFERENCES

- Ashton-James, C., van Baaren, R. B., Chartrand, T. L., Decety, J., & Karremans, J. (2007). Mimicry and me: The impact of mimicry on self-construal. *Social Cognition*, 25, 518–535.
- Astafiev, S. V., Stanley, C. M., Shulman, G. L., & Corbetta, M. (2004). Extrastriate body area in human occipital cortex responds to the performance of motor actions. *Nature Neuroscience*, 7, 542–548.
- Bahrick, L. E., & Watson, J. S. (1985). Detection of intermodal proprioceptive–visual contingency as a potential basis of self-perception in infancy. *Developmental Psychology*, 21, 963–973.
- Calvert, G. A., Campbell, R., & Brammer, M. J. (2000). Evidence from functional magnetic resonance imaging of crossmodal binding in the human heteromodal cortex. *Current Biology*, 10, 649–657.
- Caspers, S., Zilles, K., Laird, A. R., & Eickhoff, S. B. (2010). ALE meta-analysis of action observation and imitation in the human brain. *Neuroimage*, 50, 1148–1167.
- Cattaneo, L., Sandrini, M., & Schwarzbach, J. (2010). State-dependent TMS reveals a hierarchical representation of observed acts in the temporal, parietal, and premotor cortices. *Cerebral Cortex*, 20, 2252–2258.
- Chaminade, T., Meltzoff, A. N., & Decety, J. (2005). An fMRI study of imitation: Action representation and body schema. *Neuropsychologia*, 43, 115–127.
- Contaldo, A., Colombi, C., Narzisi, A., & Muratori, F. (2016). The social effect of “being imitated” in children with autism spectrum disorder. *Frontiers in Psychology*, 7, 726.
- Craig, A. D. B. (2009). Emotional moments across time: A possible neural basis for time perception in the anterior insula. *Philosophical Transactions of the Royal Society of London Series B Biological Sciences*, 364, 1933–1942.
- David, N., Cohen, M. X., Newen, A., Bewernick, B. H., Shah, N. J., Fink, G. R., et al. (2007). The extrastriate cortex distinguishes between the consequences of one's own and others' behavior. *Neuroimage*, 36, 1004–1014.
- Decety, J., Chaminade, T., Grèzes, J., & Meltzoff, A. N. (2002). A PET exploration of the neural mechanisms involved in reciprocal imitation. *Neuroimage*, 15, 265–272.
- Eickhoff, S. B., Stephan, K. E., Mohlberg, H., Grefkes, C., Fink, G. R., Amunts, K., et al. (2005). A new SPM toolbox for combining probabilistic cytoarchitectonic maps and functional imaging data. *Neuroimage*, 25, 1325–1335.
- Flandin, G., & Friston, K. J. (2017). Analysis of family-wise error rates in statistical parametric mapping using random field theory. *Human Brain Mapping*. <https://doi.org/10.1002/hbm.23839>.
- Friston, K. J., Ashburner, J. T., Kiebel, S. J., Nichols, T. E., & Penny, W. D. (2011). *Statistical parametric mapping: The analysis of functional brain images* (1st ed.). London: Academic Press.
- Friston, K. J., Harrison, L., & Penny, W. (2003). Dynamic causal modelling. *Neuroimage*, 19, 1273–1302.
- Fukushima, H., Goto, Y., Maeda, T., Kato, M., & Umeda, S. (2013). Neural substrates for judgment of self-agency in ambiguous situations. *Plos One*, 8, e72267.
- Gazzola, V., & Keysers, C. (2009). The observation and execution of actions share motor and somatosensory voxels in all tested subjects: Single-subject analyses of unsmoothed fMRI data. *Cerebral Cortex*, 19, 1239–1255.

- Gergely, G. (2001). The obscure object of desire: 'nearly, but clearly not, like me': Contingency preference in normal children versus children with autism. *Bulletin of the Menninger Clinic*, 65, 411–426.
- Gergely, G., & Watson, J. S. (1999). Early socio-emotional development: Contingency perception and the social-biofeedback model. In P. Rochat (Ed.), *Early social cognition: Understanding others in the first months of life* (pp. 101–136). New York: Psychology Press (Chapter 5).
- Giudice, M. D., Manera, V., & Keysers, C. (2009). Programmed to learn? The ontogeny of mirror neurons. *Developmental Science*, 12, 350–363.
- Guionnet, S., Nadel, J., Bertasi, E., Sperduti, M., Delaveau, P., & Fossati, P. (2012). Reciprocal imitation: Toward a neural basis of social interaction. *Cerebral Cortex*, 22, 971–978.
- Hamilton, A. F., & Grafton, S. T. (2008). Action outcomes are represented in human inferior frontoparietal cortex. *Cerebral Cortex*, 18, 1160–1168.
- Heim, S., Eickhoff, S. B., Ischebeck, A. K., Friederici, A. D., Stephan, K. E., & Amunts, K. (2009). Effective connectivity of the left BA 44, BA 45, and inferior temporal gyrus during lexical and phonological decisions identified with DCM. *Human Brain Mapping*, 30, 392–402.
- Hobson, R. P., & Lee, A. (2010). Reversible autism among congenitally blind children? A controlled follow-up study. *Journal of Child Psychology and Psychiatry*, 51, 1235–1241.
- Iacoboni, M., & Dapretto, M. (2006). The mirror neuron system and the consequences of its dysfunction. *Nature Reviews Neuroscience*, 7, 942–951.
- Keysers, C., & Gazzola, V. (2009). Expanding the mirror: Vicarious activity for actions, emotions, and sensations. *Current Opinion in Neurobiology*, 19, 666–671.
- Keysers, C., & Perrett, D. I. (2004). Demystifying social cognition: A Hebbian perspective. *Trends in Cognitive Sciences*, 8, 501–507.
- Kilner, J. M., Friston, K. J., & Frith, C. D. (2007). Predictive coding: An account of the mirror neuron system. *Cognition Processing*, 8, 159–166.
- Kitada, R., Yoshihara, K., Sasaki, A. T., Hashiguchi, M., Kochiyama, T., & Sadato, N. (2014). The brain network underlying the recognition of hand gestures in the blind: The supramodal role of the extrastriate body area. *Journal of Neuroscience*, 34, 10096–10108.
- Kontaris, I., Wiggett, A. J., & Downing, P. E. (2009). Dissociation of extrastriate body and biological-motion selective areas by manipulation of visual-motor congruency. *Neuropsychologia*, 47, 3118–3124.
- Kuhn, S., Muller, B. C., van Baaren, R. B., Wietzker, A., Dijksterhuis, A., & Brass, M. (2010). Why do I like you when you behave like me? Neural mechanisms mediating positive consequences of observing someone being imitated. *Social Neuroscience*, 5, 384–392.
- Limanowski, J., & Blankenburg, F. (2016). Integration of visual and proprioceptive limb position information in human posterior parietal, premotor, and extrastriate cortex. *Journal of Neuroscience*, 36, 2582–2589.
- Limanowski, J., Lutti, A., & Blankenburg, F. (2014). The extrastriate body area is involved in illusory limb ownership. *Neuroimage*, 86, 514–524.
- Matsuyoshi, D., Morita, T., Kochiyama, T., Tanabe, H. C., Sadato, N., & Kakigi, R. (2015). Dissociable cortical pathways for qualitative and quantitative mechanisms in the face inversion effect. *The Journal of Neuroscience*, 35, 4268–4279.
- Molenberghs, P., Cunnington, R., & Mattingley, J. B. (2012). Brain regions with mirror properties: A meta-analysis of 125 human fMRI studies. *Neuroscience and Biobehavioral Reviews*, 36, 341–349.
- Nadel, J. (2002). Imitation and imitation recognition: Functional use in preverbal infants and nonverbal children with autism. In A. N. Meltzoff, & W. Prinz (Eds.), *The imitative mind: Development, evolution and brain bases* (pp. 42–62). Cambridge: Cambridge University Press.
- Nahab, F. B., Kundu, P., Gallea, C., Kakareka, J., Pursley, R., Pohida, T., et al. (2011). The neural processes underlying self-agency. *Cerebral Cortex*, 21, 48–55.
- Okamoto, Y., Kitada, R., Tanabe, H. C., Hayashi, M. J., Kochiyama, T., Munesue, T., et al. (2014). Attenuation of the contingency detection effect in the extrastriate body area in autism spectrum disorder. *Neuroscience Research*, 87, 66–76.
- Okamoto, Y., Kosaka, H., Kitada, R., Seki, A., Tanabe, H. C., Hayashi, M. J., et al. (2017). Age-dependent atypicalities in body- and face-sensitive activation of the EBA and FFA in individuals with ASD. *Neuroscience Research*, 119, 38–52.
- Oldfield, R. C. (1971). The assessment and analysis of handedness: The Edinburgh inventory. *Neuropsychologia*, 9, 97–113.
- Oosterhof, N. N., Tipper, S. P., & Downing, P. E. (2013). Crossmodal and action-specific: Neuroimaging the human mirror neuron system. *Trends in Cognitive Sciences*, 17, 311–318.
- Orlov, T., Makin, T. R., & Zohary, E. (2010). Topographic representation of the human body in the occipitotemporal cortex. *Neuron*, 68, 586–600.
- Penny, W. D., Stephan, K. E., Daunizeau, J., Rosa, M. J., Friston, K. J., Schofield, T. M., et al. (2010). Comparing families of dynamic causal models. *PLoS Computational Biology*, 6.
- Raij, T., Uutela, K., & Hari, R. (2000). Audiovisual integration of letters in the human brain. *Neuron*, 28, 617–625.
- Reid, V. M., Striano, T., & Iacoboni, M. (2011). Neural correlates of dyadic interaction during infancy. *Developmental Cognitive Neuroscience*, 1, 124–130.
- Rizzolatti, G., Fogassi, L., & Gallese, V. (2001). Neurophysiological mechanisms underlying the understanding and imitation of action. *Nature Reviews Neuroscience*, 2, 661–670.
- Saby, J. N., Marshall, P. J., & Meltzoff, A. N. (2012). Neural correlates of being imitated: An EEG study in preverbal infants. *Social Neuroscience*, 7, 650–661.
- Sasaki, A. T., Kochiyama, T., Sugiura, M., Tanabe, H. C., & Sadato, N. (2012). Neural networks for action representation: A functional magnetic-resonance imaging and dynamic causal modeling study. *Frontiers in Human Neuroscience*, 6, 236.
- Shattuck, D. W., Mirza, M., Adisetiyo, V., Hojatkashani, C., Salamon, G., Narr, K. L., et al. (2008). Construction of a 3D probabilistic atlas of human cortical structures. *Neuroimage*, 39, 1064–1080.
- Sperduti, M., Delaveau, P., Fossati, P., & Nadel, J. (2011). Different brain structures related to self- and external-agency attribution: A brief review and meta-analysis. *Brain Structure and Function*, 216, 151–157.
- Stephan, K. E., Penny, W. D., Daunizeau, J., Moran, R. J., & Friston, K. J. (2009). Bayesian model selection for group studies. *Neuroimage*, 46, 1004–1017.
- Stephan, K. E., Penny, W. D., Moran, R. J., den Ouden, H. E. M., Daunizeau, J., & Friston, K. J. (2010). Ten simple rules for dynamic causal modeling. *Neuroimage*, 49, 3099–3109.
- Sumiya, M., Koike, T., Okazaki, S., Kitada, R., & Sadato, N. (2017). Brain networks of social action-outcome contingency: The role of the ventral striatum in integrating signals from the sensory cortex and medial prefrontal cortex. *Neuroscience Research*, 123, 43–54.
- Takahashi, H. K., Kitada, R., Sasaki, A. T., Kawamichi, H., Okazaki, S., Kochiyama, T., et al. (2015). Brain networks of affective mentalizing revealed by the tear effect: The integrative role of the medial prefrontal cortex and precuneus. *Neuroscience Research*, 101, 32–43.
- Tettamanti, M., Manenti, R., Della Rosa, P. A., Falini, A., Perani, D., Cappa, S. F., et al. (2008). Negation in the brain: Modulating action representations. *Neuroimage*, 43, 358–367.
- Tsakiris, M., Longo, M. R., & Haggard, P. (2010). Having a body versus moving your body: Neural signatures of agency and body-ownership. *Neuropsychologia*, 48, 2740–2749.

- 1 van Baaren, R. B., Holland, R. W., Kawakami, K., & van  
2 Knippenberg, A. (2004). Mimicry and prosocial behavior.  
3 *Psychological Science*, 15, 71–74.
- 4 Van Overwalle, F. (2009). Social cognition and the brain: A meta-  
5 analysis. *Human Brain Mapping*, 30, 829–858.
- 6 Werner, S., & Noppeney, U. (2010). Distinct functional  
7 contributions of primary sensory and association areas to  
8 audiovisual integration in object categorization. *The Journal of*  
9 *Neuroscience*, 30, 2662–2675.
- 10
- 11 Wold, A., Limanowski, J., Walter, H., & Blankenburg, F. (2014).  
12 Proprioceptive drift in the rubber hand illusion is intensified  
13 following 1 Hz TMS of the left EBA. *Frontiers in Human*  
14 *Neuroscience*, 8, 390.
- 15 Wurm, M. F., & Lingnau, A. (2015). Decoding actions at different  
16 levels of abstraction. *Journal of Neuroscience*, 35, 7727–7735.
- 17 Yomogida, Y., Sugiura, M., Sassa, Y., Wakusawa, K., Sekiguchi, A.,  
18 Fukushima, A., et al. (2010). The neural basis of agency: An  
19 fMRI study. *Neuroimage*, 50, 198–207.
- 20

UNCORRECTED PROOF